Frequency Domain Iterative Feedforward/Feedback Tuning for MIMO ANVC ⋆

Jian Luo [a], Sandor M. Veres [a],

[a] *School of Engineering Sciences, University of Southampton, Highfield, Southampton, SO17 1BJ United Kingdom*

Abstract

A new gradient estimation method is proposed that relies on efficient computation of the negative gradient of the average linear quadratic cost function completely in the frequency domain. Based on the proposed theory, a new iterative tuning method is developed to solve linear multi-input multi-output Active Noise/Vibration Control problems. Compared with published iterative tuning methods, the new method has the added advantage that the number of experiments per iteration is reduced to one. Combined with the other advantage of relatively simple controller structures, the method is suitable for real-time implementation as an adaptive controller.

Key words: Self-tuning control; Feedback/feedforward control; Iterative method; Active noise/vibration control; Frequency domains; MIMO systems.

1 Introduction

Iterative feedback tuning (IFT) has been the subject of intensive research effort during the past decade [3,4,6,5]. Its advantage is that it does not need detailed plant modelling, assuming that a stable reasonably functioning controller is available to start with. Recent efforts were aimed at improving gradient estimation [9,8] of the control performance criterion and improving stability robustness without modelling [23].

This paper extends work in [12] to propose a new gradient estimation method in the frequency domain to deal with adaptive control problems in Multi-Input Multi-Output (MIMO) systems, which relies on the analysis of frequency response of the system dynamics and spectrum of signals. With local linearization analysis techniques in the frequency domain, the key to this solution is the investigation of the mapping from the change of control parameters to the change of output spectra.

Using this technique a new Iterative Tuning (IT) method in the Frequency domain (FD), i.e., FD-IT, is developed for linear MIMO control problems with periodic signals. It is a data-driven approach which only requires partial modelling according to the discrete spectrum of signals. It is applicable to a variety of controller structures, including finite-impulse-response (FIR) model based and frequency-selective-filter (FSF) based controllers. One initial experiment is required for each input channel of the unknown plant to initialize the gradient estimate. Later tuning takes place simultaneously for all inputs while the iterative feedback/feedforward tuning in earlier publications [4] had to perform multiple experiments for feedback and feedforward controllers.

The proposed gradient estimation method is applicable to general control problems, including nonlinear ones, as the gradient approximation approach is valid for nonlinear systems. Despite this generality, the proposed tuning method is specialized to the LTI case with periodic signals for ease of implementation as the general case is computationally intensive. The most important target area of its application is Active Noise and Vibration Control (ANVC) problems which often need to attenuate the effect of periodic disturbances. Many methods have been developed for ANVC during the past twenty years. There are design approaches that are model-based, e.g., H_∞ control [2], unfalsification control [24] and correlation based IFT [11]. There are many model-free approaches as well. One of the most widely used and well understood methods is the filtered-x LMS algorithm [18], which can be made adaptive to track plant dynamics with slow time variance. Frequency selective filter-based iterative feedback/feedforward tuning (FSF-IFT) control [16] has also been successfully used for periodic disturbance cancelation. There are very few effective methods available to tune both feedback/feedforward controllers in ANVC. This paper suggests a method of tuning feedback

⋆ An early version of this paper was presented at ALCOSP'07. Corresponding author S. M. Veres.

Email addresses: luoj@soton.ac.uk (Jian Luo), s.m.veres@soton.ac.uk (Sandor M. Veres).

and feed-forward controllers simultaneously.

The remainder of this paper is organized as follows. In Section 2, the problem of gradient-based tuning control for ANVC is shortly reviewed in the time domain and reformulated in the frequency domain. In Section 3 the gradient estimation method is proposed and the new iterative tuning method (FD-IT) is developed in Section 4. Section 5 compares FD-IT to some other iterative tuning methods in the time domain. In Section 6 a series of MIMO simulation examples are presented to compare two implementations of FD-IT and the robustness of the algorithm. Finally conclusions are drawn in the last section.

2 Gradient based tuning for ANVC

In this section, the ANVC problem is addressed in the time domain and frequency domain in general, fundamental definitions and the performance function are given and the essence of iterative tuning is formulated in the context of the ANVC problem.

2.1 Problem setting in the time domain

Figure 1 provides a schematic description of the control system considered.

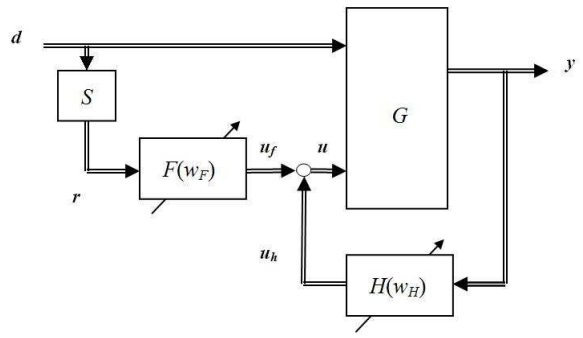

Fig. 1. Block diagram of the linear feedforward/feedback ANVC system.

The measured output, which is affected by the disturbance $\boldsymbol{d} \in \mathbb{R}^{n_d}$, is represented by $\boldsymbol{y} \in \mathbb{R}^{n_y}$. G is the unknown plant dynamics with inputs $\boldsymbol{d}$ and $\boldsymbol{u}$ and produces the vector output $\boldsymbol{y}$. It can be described as

$$\boldsymbol{y} = G(\boldsymbol{d}, \boldsymbol{u}) \tag{1}$$

The control signals from the feedforward controller F and feedback controller H are denoted by $\boldsymbol{u}_f \in \mathbb{R}^{n_u}$ and $\boldsymbol{u}_h \in \mathbb{R}^{n_u}$, respectively. The tunable control system C comprises the parameterized feedforward controller F and the feedback controller H:

$$\begin{aligned} C(\boldsymbol{w}, \boldsymbol{r}, \boldsymbol{y}): \quad F: \boldsymbol{u}_f &= F(\boldsymbol{w}_F, \boldsymbol{r}) \\ H: \boldsymbol{u}_h &= H(\boldsymbol{w}_H, \boldsymbol{y}) \\ \boldsymbol{u} &:= \{\boldsymbol{u}_f, \boldsymbol{u}_h\} \end{aligned} \tag{2}$$

which can be tuned by adjusting their parameter vectors in $\boldsymbol{w} := \{\boldsymbol{w}_F, \boldsymbol{w}_H\} \in \mathbb{R}^{n_w}$.

As usual in ANVC, it is assumed that the measurable disturbance-reference signal $\boldsymbol{r} \in \mathbb{R}^{n_r}$ is correlated to disturbance $\boldsymbol{d}$, and $\boldsymbol{r}$ is obtained through an unknown but time-invariant dynamics S from $\boldsymbol{d}$. While the output signal $\boldsymbol{y}(t)$ is measurable and recordable, the disturbance signal $\boldsymbol{d}$ cannot be measured directly.

In the case of a periodic disturbance $\boldsymbol{d}$, it is always assumed that the steady output $\boldsymbol{y}$ is also periodic. If the system has steady output $\boldsymbol{y}$ with period N then the control performance criterion is defined as the average quadratic performance of a length N output sequence:

$$J(\boldsymbol{w}) := \frac{1}{N} \sum_{t=0}^{N-1} \boldsymbol{y}^{\mathrm{T}}(t) Q \boldsymbol{y}(t) \tag{3}$$

where Q is a priori specified weighting matrix.

The objective of tuning for ANVC is to adjust the controller parameters $\boldsymbol{w}_F$ and $\boldsymbol{w}_H$ to minimize the performance criterion (3).

In general, the problem of minimizing $J(\boldsymbol{w}_F, \boldsymbol{w}_H)$ is not necessarily convex. The tuning method often finds a suboptimal solution at a local minimum. This suboptimal solution of the problem is obtained by finding $\boldsymbol{w}^o = \{\boldsymbol{w}_F^o, \boldsymbol{w}_H^o\}$ that satisfies

$$\nabla J(\boldsymbol{w}_F^o, \boldsymbol{w}_H^o) = \boldsymbol{0} \tag{4}$$

On the topic of how to solve the global optimization problem, there are a number of papers available [21,20,22,1] as referenced.

2.2 Problem setting in the frequency domain

In this subsection the ANVC problem as in Fig.1 and with cost function (3) will be represented in the frequency domain.

Considering the MIMO system described by Fig.1, if there is N-length output data set $\mathscr{Y} := \{\boldsymbol{y}(0); \ldots; \boldsymbol{y}(N-1)\}, \boldsymbol{y}(t) := \{y_1(t), \ldots, y_{ny}(t)\} \in \mathrm{R}^{n_y}$, this can be detailed with the output channels as $\mathscr{Y} = \{\boldsymbol{y}_1, \ldots, \boldsymbol{y}_{n_y}\}, \boldsymbol{y}_i = \{y_i(0); \ldots; y_i(N-1)\}, i = 1, \ldots, n_y$.

Denoting by $\Omega_N = \{\omega_m := m\frac{2\pi}{N}, m = 0, \ldots, N-1\}$ the set of uniformly sampled discrete frequencies for N-length data,

$\boldsymbol{\phi}_y^i := \{\phi_y^i(\omega_0); \ldots; \phi_y^i(\omega_{N-1})\} \in \mathbb{C}^N$ will be the notation for the Discrete Fourier Transform (DFT), that is a windowless estimate of the discrete spectrum of $\boldsymbol{y}_i$, i.e. $\boldsymbol{\phi}_y^i \doteq \mathrm{DFT}(\boldsymbol{y}_i)$. Furthermore, the discrete spectrum of $\mathscr{Y}$ is presented as $\boldsymbol{\phi}_y := \{\boldsymbol{\phi}_y^1; \ldots; \boldsymbol{\phi}_y^{n_y}\} \in \mathbb{C}^{(n_y \cdot N) \cdot 1}$. There are some similar further notations such as $\boldsymbol{\phi}_d$, $\boldsymbol{\phi}_r$, $\boldsymbol{\phi}_{uf}$ and $\boldsymbol{\phi}_{uh}$.

In the frequency domain, the plant G is described as a mapping: $\{\boldsymbol{\phi}_d, \boldsymbol{\phi}_u\} \in \mathbb{C}^{(n_d \cdot N + n_u \cdot N)} \mapsto \boldsymbol{\phi}_y \in \mathbb{C}^{(n_y \cdot N)}$:

$$\boldsymbol{\phi}_y = \Phi_G(\boldsymbol{\phi}_d, \boldsymbol{\phi}_u) = \Phi_G(\boldsymbol{\phi}_d, \boldsymbol{\phi}_u^1, \ldots, \phi_u^{n_u}), \tag{5}$$

and the controller system C is described as a mapping: $\{\boldsymbol{w}, \boldsymbol{\phi}_r, \boldsymbol{\phi}_y\} \in \mathbb{C}^{(n_w + n_r \cdot N + n_y \cdot N)} \mapsto \boldsymbol{\phi}_u \in \mathbb{C}^{(n_y \cdot N)}$:

$$\begin{aligned} \Phi_C(\boldsymbol{w}, \boldsymbol{\phi}_r, \boldsymbol{\phi}_y): \quad \Phi_F : \boldsymbol{\phi}_{uf} &= \Phi_F(\boldsymbol{w}_F, \boldsymbol{\phi}_r) \\ \Phi_H : \boldsymbol{\phi}_{uh} &= \Phi_H(\boldsymbol{w}_H, \boldsymbol{\phi}_y) \\ \boldsymbol{\phi}_u &:= \{\boldsymbol{\phi}_{uf}, \boldsymbol{\phi}_{uh}\} \end{aligned} \tag{6}$$

According to Parseval's Theorem [19], it is straightforward to rewrite (3) in the frequency domain format as

$$J = \frac{1}{N} \sum_{i=0}^{N-1} \phi_y^*(\omega_i) \Phi_Q \phi_y(\omega_i) = \frac{1}{N^2} \boldsymbol{\phi}_y^* \Phi_Q \boldsymbol{\phi}_y \tag{7}$$

where Φ_Q is the representation of Q in the frequency domain.

Similarly, the optimization problem can be written as:

$$\begin{aligned} \min: \ & J(\boldsymbol{w}) \text{ in (7)}, \\ s.t. \quad & \text{Eqn. (5)}, \\ & \text{Eqn. (6)}. \end{aligned} \tag{8}$$

Note that the system as Fig.1 is represented in the frequency domain as general mappings between two multi-dimensional spaces, and the cost function (3) is also represented in the frequency domain as multiplication of discrete spectra. This representation is suitable to describe general systems including linear or nonlinear ones.

3 Gradient estimation in the frequency domain

In this section, a new gradient estimation theory is proposed, from a frequency domain aspect, which is based on the reformatted ANVC problem as presented above.

3.1 Gradient estimation in full-bandwidth

In a gradient-based algorithm the continuous differentiability condition is always necessary. Similarly, in iterative tuning in the frequency domain, it is also assumed that Φ_G, Φ_F and Φ_H are continuously differentiable functions with respect to their input spectra and tunable parameters. In order to discover the relationship between control performance and control parameters, local linearization can be performed and computed using infinitesimal increments.

Considering the ANVC system in Fig. 1, the local linearisation of Φ_G can be described as

$$\Delta\boldsymbol{\phi}_y \approx \frac{\mathrm{d}\boldsymbol{\phi}_y}{\mathrm{d}\{\boldsymbol{\phi}_d, \boldsymbol{\phi}_u\}} \begin{bmatrix} \Delta\boldsymbol{\phi}_d \\ \Delta\boldsymbol{\phi}_u \end{bmatrix} \tag{9}$$

As the $\boldsymbol{\phi}_d$ is fixed for stationary disturbances, only the case of $\Delta\boldsymbol{\phi}_d = \boldsymbol{0}$ is needed to be discussed. To simplify the presentation, some of the most frequently used notations are defined as

$$\Phi_{G'} := \frac{\partial \boldsymbol{\phi}_y}{\partial \boldsymbol{\phi}_u} \in \mathbb{C}^{(n_y \cdot N) \cdot (n_u \cdot N)}, \tag{10}$$

and similarly

$$\Phi_{H'} := \frac{\boldsymbol{\phi}_{uh}}{\partial \boldsymbol{\phi}_y} \in \mathbb{C}^{(n_{uh} \cdot N*) \cdot (n_y \cdot N)} \tag{11}$$

Without losing generality, given $\boldsymbol{\phi}_y$, $\boldsymbol{\phi}_u$ and $\Phi_{G'}$, the infinitesimal increment format of dynamics G in the frequency domain with respect to $\Delta\boldsymbol{\phi}_u$ can be written as

$$\Delta\boldsymbol{\phi}_y \approx \Phi_{G'}(\Delta\boldsymbol{\phi}_{uf}^w + \Delta\boldsymbol{\phi}_{uh}^w) \tag{12}$$

For the tunable controllers $\Phi_F(\boldsymbol{w}_F, \boldsymbol{\phi}_r)$ and $\Phi_H(\boldsymbol{w}_H, \boldsymbol{\phi}_y)$ in (6), the following notations are going to be used:

$$\Phi_{F'}^w := \frac{\partial \boldsymbol{\phi}_{uf}}{\partial \boldsymbol{w}_F} \in \mathbb{C}^{(n_u \cdot N) \cdot n_{wF}}, \Phi_{H'}^w := \frac{\partial \boldsymbol{\phi}_{uh}}{\partial \boldsymbol{w}_H} \in \mathbb{C}^{(n_u \cdot N) \cdot n_{wH}} \tag{13}$$

Considering small increments caused by the small update of parameter $\boldsymbol{w}$, i.e., $\boldsymbol{w}_F \to \boldsymbol{w}_F + \Delta\boldsymbol{w}_F$ and $\boldsymbol{w}_H \to \boldsymbol{w}_H + \Delta\boldsymbol{w}_H$, it is straightforward to write

$$\Delta\boldsymbol{\phi}_y \approx \Phi_{G'}(\Phi_{F'}^w \Delta\boldsymbol{w}_F + \Phi_{H'}^w \Delta\boldsymbol{w}_H + \Phi_{H'}^w \Delta\boldsymbol{\phi}_y) \tag{14}$$

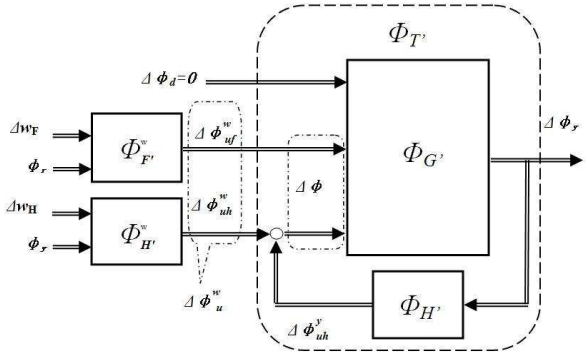

Fig. 2. Block diagram of small increment in frequency domain.

Using notations that $\Delta\boldsymbol{\phi}^w_{uf} \approx \Phi^w_{F'}\Delta\boldsymbol{w}_F$, $\Delta\boldsymbol{\phi}^w_{uh} \approx \Phi^w_{H'}\Delta\boldsymbol{w}_H$ and $\Delta\boldsymbol{\phi}^y_{uh} \approx \Phi_{H'}\Delta\boldsymbol{\phi}_y$, (14) can be graphically described by Fig. 2.

The input/output increment mapping is $\Delta\boldsymbol{\phi}_u \mapsto \Delta\boldsymbol{\phi}_y$. The physical increment in the path of the feedback controller H consists of two parts: $\Delta\boldsymbol{\phi}^w_{uh}$ caused by the change of controller parameter $\Delta\boldsymbol{w}_H$, and $\Delta\boldsymbol{\phi}^y_{uh}$ caused by the change of output $\Delta\boldsymbol{\phi}_y$.

Considering that the part $\Delta\boldsymbol{\phi}_u$ is only caused by the Δw, if $(I-\Phi_{G'}\Phi_{H'})^{-1}$ exists, the input/output mapping $\{\Delta\boldsymbol{\phi}^w_{uf}, \Delta\boldsymbol{\phi}^w_{uh}\} \mapsto \Delta\boldsymbol{\phi}_y$ can be rewritten from (14) as

$$\Delta\boldsymbol{\phi}_y \approx (I-\Phi_{G'}\Phi_{H'})^{-1}\Phi_{G'}(\Delta\boldsymbol{\phi}^w_{uf}+\Delta\boldsymbol{\phi}^w_{uh}) \tag{15}$$

By introducing the notation

$$\Phi_{T'} := (I-\Phi_{G'}\Phi_{H'})^{-1}\Phi_{G'} \in \mathbb{C}^{(n_y\cdot N)\cdot(n_u\cdot N)}, \tag{16}$$

the key result turns out to be that the derivative of $\boldsymbol{\phi}_y$ with respect to controller parameters $\boldsymbol{w}_H$ and $\boldsymbol{w}_F$ can be approximated as

$$\frac{\partial\boldsymbol{\phi}_y}{\partial\boldsymbol{w}_F} \approx \Phi_{T'}\Phi_{F'}, \quad \frac{\partial\boldsymbol{\phi}_y}{\partial\boldsymbol{w}_H} \approx \Phi_{T'}\Phi_{H'} \tag{17}$$

The derivative of performance J with respect to controller parameters can be written in the frequency domain as

$$\frac{\partial J(\boldsymbol{w})}{\partial\boldsymbol{w}} \approx \frac{2}{N^2}\boldsymbol{\phi}^*_y\Phi_Q\Phi_{T'}\frac{\partial\Phi_C}{\partial\boldsymbol{w}} \tag{18}$$

Generally, the output $\boldsymbol{y}$, the controller H and F are all known, $\boldsymbol{\phi}_y$ and

$$\frac{\partial\Phi_C}{\partial\boldsymbol{w}} = [\Phi_{F'},\ \Phi_{H'}]$$

can be both estimated. The final point of to gradient estimation is the approximate computation of $\Phi_{T'}$ at the relevant frequencies that will add an initial experiment to our procedure.

Remark 1 *As mentioned at the beginning of this section, the above deduction is completely based on the representation in the frequency domain without considering time domain. But the conclusions are similar to IFT results in the time domain [3], which may point to similar conclusions in other integral transform domains, i.e., wavelet transform domain in a future research.*

Remark 2 *Note that the above deduction is based on a local linearization analysis with incremental equation (12). If nonlinear G and C have continuous derivative matrices in the frequency domain (i.e., $\Phi_{G'}$, $\Phi_{C'}$), then the derivation in the nonlinear case is straightforward as discussed in [13].*

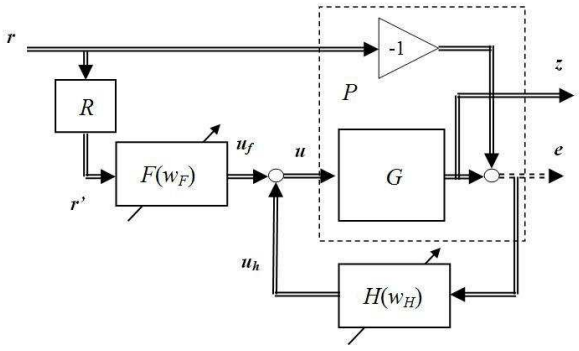

Fig. 3. Block diagram of a servo control problem.

Remark 3 *Although Fig.1 illustrates ANVC, it can be used to present common control problems with some slight modifications. As shown in Fig. 3, a servo control problem can be illustrated with a similar format of ANVC, where '$\boldsymbol{d}$' and $\boldsymbol{y}$ is replaced by $\boldsymbol{r}$ and $\boldsymbol{e}$ in Fig. 3, respectively. In [14], the proposed idea has been adopted to implement a tracking control problem. Therefore, the proposed gradient estimate as (18) is valid in theory for most of general control problems with a periodic reference signal.*

3.2 Gradient estimate in finite frequency set

In the subsection above (18) gives a full-bandwidth format in the frequency domain including the full-band from ω_0 to ω_{N-1}. However, the computation of the performance gradient can be greatly simplified in LTI systems with periodic disturbances that cover only part of the full-bandwidth.

Note that in (18) $\boldsymbol{\phi}^*_y$ can be considered as a weighting sequence when it is rewritten as

$$\frac{\partial J(\boldsymbol{w})}{\partial\boldsymbol{w}} \approx \frac{2}{N^2}\sum_{n=0}^{N-1}\phi^*_y(\omega_n)\Phi_Q(\omega_n)\frac{\partial\phi_y(\omega_n)}{\partial\boldsymbol{w}} \tag{19}$$

Considering periodic output $\boldsymbol{y}$ with common period N and finite frequency set

$$\Omega := \{\bar{\omega}_0, \ldots, \bar{\omega}_n\} \subset \Omega_N$$

$\boldsymbol{\phi}_y$ can be substituted with $\boldsymbol{\phi}_y|_\Omega$, and the other elements in $\boldsymbol{\phi}_y$ are 0. Therefore, in order to get $\frac{\partial J(\boldsymbol{w})}{\partial \boldsymbol{w}}$ in (18), only the elements in $\frac{\partial \boldsymbol{\phi}_y}{\partial \boldsymbol{w}}$ with respect to Ω are required to be included, i.e.,

$$\frac{\partial J(\boldsymbol{w})}{\partial \boldsymbol{w}} \approx \frac{2}{N^2} \sum_{\omega \in \Omega} \phi_y^*(\omega) \Phi_Q(\omega) \frac{\partial \phi_y(\omega)}{\partial \boldsymbol{w}} \tag{20}$$

In this case only the partial dynamics $\{\Phi_{T'} \frac{\partial \phi_C}{\partial \boldsymbol{w}}\}|_\Omega$ is required to be estimated according to the frequency domain characteristics of $\boldsymbol{y}$. (20) provides a data-driven approach to tune the controller that only requires partial modelling according to the discrete spectrum of signals. If $\{\Phi_{T'} \frac{\partial \phi_C}{\partial \boldsymbol{w}}\}|_\Omega$ has some easy presentation then the computation of $\nabla J(\boldsymbol{w})$ can be simplified.

Fortunately, in LTI systems there is a very simple presentation in the frequency domain: the frequency response is independent for individual frequencies, and in this case, $\frac{\partial \phi_y(\omega)}{\partial \boldsymbol{w}}$ can be decomposed as

$$\frac{\partial \phi_y(\omega)}{\partial \boldsymbol{w}} \approx \Phi_T(\boldsymbol{\phi}_u(\omega), \boldsymbol{\phi}_d(\omega)) \frac{\partial \Phi_C(\boldsymbol{w}, \boldsymbol{\phi}_r(\omega), \boldsymbol{\phi}_y(\omega))}{\partial \boldsymbol{w}}$$

.

Therefore, in LTI systems, it is straightforward to rewrite (18) to the format with respect to the finite frequency set Ω as

$$\frac{\partial J(\boldsymbol{w})}{\partial \boldsymbol{w}} \approx \frac{2}{N} \boldsymbol{\phi}_y^*|_\Omega \Phi_Q|_\Omega \Phi_T|_\Omega \frac{\partial \Phi_C(\boldsymbol{w}, \boldsymbol{\phi}_r, \boldsymbol{\phi}_y)}{\partial \boldsymbol{w}}|_\Omega \tag{21}$$

In this case, the advantage of gradient estimate in the frequency domain is explicit: while the problem in the time domain is to solve N sub-problems for estimating $\frac{\partial y(t)}{\partial \boldsymbol{w}}, t = 0, \ldots, N-1$, the problem in the frequency domain is to solve n sub-problems of estimation of $\frac{\partial \phi_y|_{\omega_i}}{\partial \boldsymbol{w}}, i = 0, \ldots, n$. Therefore, the gradient computation can be greatly simplified when $N >> n$.

4 Iterative Tuning in the Frequency Domain

In this section a new iterative tuning method is developed for linear MIMO ANVC problems with periodic disturbances.

4.1 Tuning a MIMO system in the frequency domain

In (21), the key to approximating $\frac{\partial J(\boldsymbol{w})}{\partial w}$ is to estimate the derivative matrix $\Phi_T|_\Omega$, which has $((n_y \cdot n_u) \cdot n)$ unknown variables in LTI case.

In LTI systems the Frequency Response Function (FRF) matrix is independent of the frequency ω. To ease the description, the single frequency FRF of Φ_T, i.e., $\Phi_T|_\omega$), is used in the following discussion, and the extension to all relevant frequencies is straightforward. Recalling (16), if $\Phi_{G'}$ can be estimated, $\Phi_{T'}$ can also be estimated since H is known:

$$\hat{\Phi}_T|_\omega = (I - \hat{\Phi}_{G|_\omega} \Phi_{H|_\omega})^{-1} \hat{\Phi}_{G|_\omega} \in \mathbb{C}^{(n_y \cdot n_u)} \tag{22}$$

where hats $\hat{*}$ are used for estimates.

Applying two linear controllers $\{F(\boldsymbol{w}_F^i), H(\boldsymbol{w}_H^i)\}$ and $\{F(\boldsymbol{w}_F^j), H(\boldsymbol{w}_H^j)\}$ to the linear system in Fig. 1, the control action, reference signal and output are $\boldsymbol{u}_{uf}^i$ and $\boldsymbol{u}_{uf}^j$, $\boldsymbol{u}_{uh}^i$ and $\boldsymbol{u}_{uh}^j$, $\boldsymbol{r}^i$ and $\boldsymbol{r}^j$, $\boldsymbol{y}^i$ and $\boldsymbol{y}^j$, respectively. Note that the underlying ϕ_r^i and ϕ_r^j are required to keep identical phases. The output increment is approximated by

$$\Delta \boldsymbol{\phi}_y^{\{i,j\}}(\omega) \approx \Phi_G|_\omega \Delta \boldsymbol{\phi}_u^{\{i,j\}}(\omega), \tag{23}$$

where $\Delta \boldsymbol{\phi}_y^{\{i,j\}}(\omega) := \boldsymbol{\phi}_y^i(\omega) - \boldsymbol{\phi}_y^j(\omega)$ and $\Delta \boldsymbol{\phi}_u^{\{i,j\}}(\omega) := \boldsymbol{\phi}_u^i(\omega) - \boldsymbol{\phi}_u^j(\omega)$. While $\Phi_G|_\omega$ has $(n_y \cdot n_u)$ unknown variables, (23) gives n_y equations. Given n_u pairs of difference data $\{\Delta \boldsymbol{u}, \Delta \boldsymbol{y}\}$ to set up n_u such different equation groups as (23), the estimate $\hat{\Phi}_G|_\omega$ can be computed from $(n_u \cdot n_y)$ equations in (23). Using $\hat{\Phi}_G|_\omega$ the $\hat{\Phi}_T|_\Omega$ can be computed using (22) and $\nabla J(\boldsymbol{w})$ can be obtained by (21). Therefore, the gradient $\nabla J(\boldsymbol{w})$ can be estimated through $(n_u + 1)$ experiments in the case of LTI systems.

4.2 Implementation of FD-IT

For LTI systems, $\Phi_G|_\omega$ is considered stationary and can be estimated through initial $1 + n_u$ experiments. Using $\hat{\Phi}_G|_\omega$ and H the varying $\hat{\Phi}_T^i|_\omega$ can be computed. To make N_T gradient tuning steps, the number of experiments is $N_T + n_u$. The general algorithm of FD-IT for one step is described in Figure 4.

To implement FD-IT, the format of tunable controllers $C = \{F, H\}$ can vary as ARMA format, Numerator-Denominator (N-D) format, Zeros-Poles-Gains (Z-P-K) format and state equation format, that can be chosen by the designer according to individual requirement. FIR controllers are one of the most convenient controller structures to realize. For simple ANVC application with few frequencies, especially single frequency control, an FIR based FD-IT controller can give satisfying tuning result with a simple controller structure.

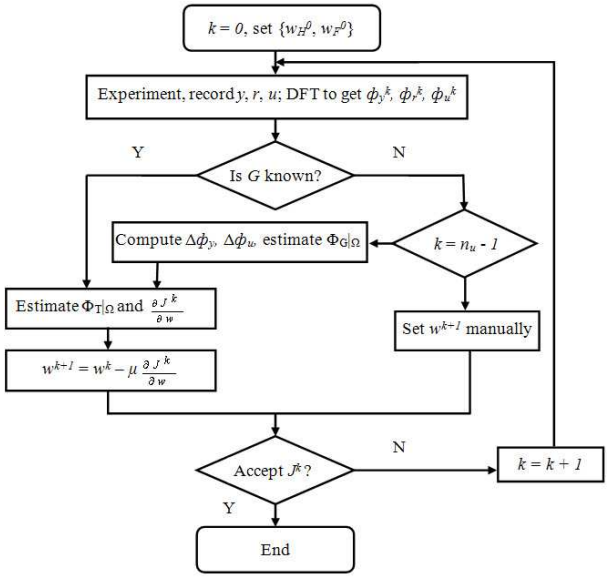

Fig. 4. A possible algorithm of FD-IT for linear systems, where k is the index of the periodic cycles, μ is an empirical adaptation gain; the rest of the notations are as defined in the text.

In order to achieve higher cancellation levels and robust tuning performance, Frequency-Selective-Filters (FSFs)[17] can be introduced for each important disturbance frequency

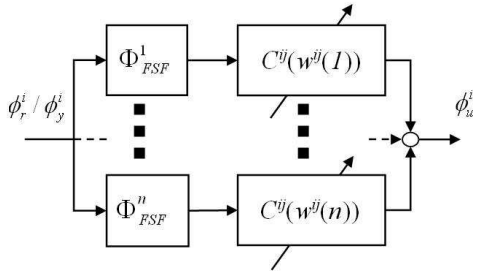

Fig. 5. Block diagram in frequency domain of one sub-block in the FSF controller

Figure 5 shows the typical block diagram of one sub-block in the FSF based controller with n FSF channels, which is from i-th input to j-th output. For the finite set of $\Omega = \{\omega_1, \ldots, \omega_n\}$, there are n_Ω FSF channels. Φ^m_{FSF} is FRF of the band-pass FSF with central frequency ω_m serial-connected with a tunable complex gain module $w^{ji}(m)$, where $m = 1, \ldots, n$.

5 Comparison with other control method

In this section, the comparison with iterative tuning methods in time domain will be discussed.

5.1 Comparison with IFT in the time domain

Time domain (TD) IFT had initially been proposed for instance in [7]. In [16] TD-IFT was introduced to control an ANVC system and has been tested in laboratory experiments [15]. It has similar physical dynamics to FD-IT, while TD-IFT can be well explained by FD-IT in the frequency domain.

To ease the description, the idea of TD-IFT is described here for the SISO case. With the LTI assumption, the key idea of TD-IFT is to estimate the derivatives of $y(t)$ with respect to $\boldsymbol{w}_H$ with [7]:

$$\boldsymbol{z}_H := \frac{\partial y(t)}{\partial \boldsymbol{w}_H} = \frac{\partial H(\boldsymbol{w}_H)}{\partial \boldsymbol{w}_H} \frac{G}{1-GH} y(t) \tag{24}$$

In [16], the estimation of the derivatives of $y(t)$ with respect to $\boldsymbol{w}_F$ is given by

$$\boldsymbol{z}_F := \frac{\partial y(t)}{\partial \boldsymbol{w}_F} = \frac{\partial F(\boldsymbol{w}_F)}{\partial \boldsymbol{w}_F} \frac{G}{1-GH} r(t) \tag{25}$$

Given the average quadratic performance criterion J as $J(\boldsymbol{w}) := \frac{1}{N}\sum_{t=0}^{N-1} y^2(t)$

it is straightforward to write

$$\frac{\partial J}{\partial \boldsymbol{w}_H} = \frac{2}{N}\sum_{t=0}^{N-1} y(t) z_H(t) \tag{26}$$

and

$$\frac{\partial J}{\partial \boldsymbol{w}_F} = \frac{2}{N}\sum_{t=0}^{N-1} y(t) z_F(t) \tag{27}$$

Injecting $\boldsymbol{y}$ and $\boldsymbol{r}$ to the closed loop system, $\frac{\partial y(t)}{\partial \boldsymbol{w}_H}$ and $\frac{\partial y(t)}{\partial \boldsymbol{w}_F}$ are the output of close-loop system $\frac{G}{1-GH}$ followed by post-filters $\frac{\partial H(\boldsymbol{w}_H)}{\partial \boldsymbol{w}_H}$ and $\frac{\partial F(\boldsymbol{w}_F)}{\partial \boldsymbol{w}_F}$, respectively.

In TD-IFT the gradient estimation of the control cost function can be achieved directly using data from additional experiments.

Comparing (17) with (24) and (25), FD-IT can be considered as having similar expression to TD-IFT in the frequency domain. They both describe the physical essence of the chain rule about the derivative, i.e., $\boldsymbol{w} \Rightarrow \boldsymbol{u} \Rightarrow \boldsymbol{y} \Rightarrow J$.

Despite the similarity of physical dynamics, TD-IFT and FD-IT is quite different in the implementation. While the additional signal injections in the extra gradient experiments are necessary to 'produce' $\frac{\partial \boldsymbol{y}}{\partial \boldsymbol{w}}$ in TD-IFT, $\frac{\partial \boldsymbol{y}}{\partial \boldsymbol{w}}$ is 'estimated' through the difference of $\boldsymbol{\phi}_y$ and $\boldsymbol{\phi}_u$ in different iterations. This difference can be produced by either additional signal injections or the change of the controller parameters. The direct advantage of FD-IT is that it gives a simpler structure without the path to inject additional signals.

Another obvious advantage of FD-IT over TD-IFT is that FD-IT requires much less iterations to tune than TD-IFT. As stated in [3,4,8], to estimate the gradient with respect to all possible parameters, $n_u \cdot n_y$ gradient experiments are necessary for the feedback controller H and $n_u \cdot n_r$ gradient experiments for feed forward controller F, which gives $(1+n_u \cdot n_y + n_u \cdot n_r)$ experiments in order to compute all gradients for one tuning step. If the blocks of the controller are not independently parameterized, a more elaborate procedure is required [3]. Figure 6 illustrates the relationship between experiments and tuning iterations for TD-IFT.

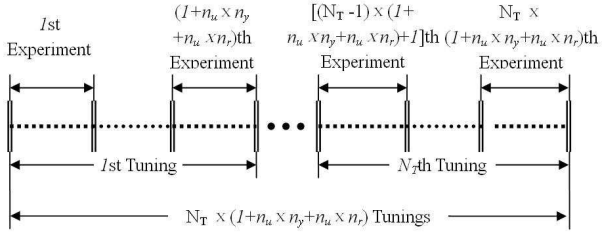

Fig. 6. Experiments and iterations in TD-IFT

On the other hand, as shown in Figure 7, FD-IT can perform N_T times tuning steps with only $N_T + n_u$ experiments, for which TD-IFT requires $N_T \cdot (1+n_u \cdot n_y + n_u \cdot n_r)$ experiments.

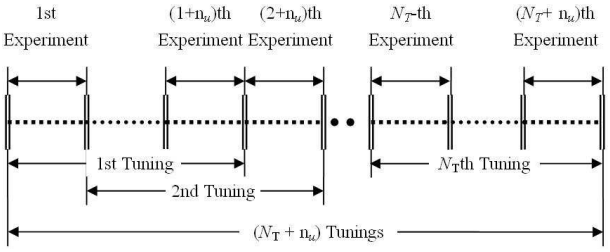

Fig. 7. Experiments and iterations in FD-IT

5.2 Comparison with direct IFT methods via spectrum analysis

In [10] a method, referred to as Direct IFT via Spectrum Analysis (SA-IFT), has been proposed to compute derivatives of linear quadratic (LQ) cost functions J with respect to the controller parameter vector $\boldsymbol{w}$ via spectral analysis of the closed loop experimental data. In this subsection FD-IT is compared to SA-IFT.

SA-IFT approaches TD-IFT via the power spectrum analysis of $\boldsymbol{y}$, i.e., $\boldsymbol{\phi}_y := \boldsymbol{\phi}_y^* \boldsymbol{\phi}_y$. SA-IFT obtains the derivative of J with respect to $\boldsymbol{w}$ as

$$\frac{\partial J}{\partial w_i} = 2\bar{\boldsymbol{\phi}}_y \mathfrak{Re}\left(\frac{G}{1+GH}\frac{\partial C}{\partial w_i}\right) \tag{28}$$

where $\mathfrak{Re}(\cdot)$ denotes the real part of complex variables. There are two unknown items in (28). One is $\bar{\boldsymbol{\phi}}_y$, which is 'produced' by a 'normal operation' that the reference signal $\boldsymbol{r}$ is assumed to be kept identically zero. Another is $\frac{G}{1+GH}$, which 'can be obtained via an intrusive experiment performed in the loop by injecting the stationary non-degenerate signal $\{r_t\}$' [10] according the following relationship:

$$\frac{\Phi_G}{1+\Phi_G\Phi_H} = \frac{\Delta\boldsymbol{\phi}_y}{\Phi_F \Delta\boldsymbol{\phi}_r}. \tag{29}$$

First of all, although (28) gives almost the same mathematical expression as (21), (28) has no explicit expression in the frequency domain to explain $\frac{\partial y(t)}{\partial \boldsymbol{w}_C}$ and the extra gradient experiments in TD-IFT because the spectrum density $\boldsymbol{\phi}_y$ is integrated into the power spectrum $\bar{\boldsymbol{\phi}}_y$ in (28). In principle, FD-IT could be viewed as a more proper frequency domain explanation of TD-IFT than SA-IFT.

Secondly, SA-IFT is quite different from FD-IT in the implementation. Since the power spectrum $\boldsymbol{\phi}_y$ in (28) varies with the change of H, in every tuning step $\bar{\boldsymbol{\phi}}_y$ should be 'produced' by a 'normal operation' that is difficult to implement in real time tuning. Additionally, SA-IFT requires an extra 'intrusive experiment' to yield $\frac{\Phi_G}{1+\Phi_G\Phi_H}$, which varies with the tuning of H. Therefore, SA-IFT always requires two experiments for one gradient estimation, i.e., 'normal operation' and 'intrusive experiment'.

6 Simulation

This section illustrates the usefulness of the FD-IT as tested in simulation using MATLAB®. FIR control structure and FSF controllers are tested and compared. The robustness to errors in the frequency estimates of the disturbance are discussed within this simulation example.

6.1 Simulation platform

The block diagram of the SIMULINK®-based simulation is given in Fig. 8. It is a 2-input and 2-output LTI system. Outports $y1$, $y2$, $r1$ and $r2$ denote the data acquiring output and reference signals. Modules $Ny1$, $Ny2$, $Nr1$ and $Nr2$ denote the sensor noise in the output and reference paths. They are assumed as being white noise with variance $1e-6$.

Figure 9 illustrates the block diagram of the unknown plant G.

In Fig. 9, control path G_u and disturbance path G_d are given by

$$G_u(q) = \begin{bmatrix} \frac{0.1q^{-8}-0.3q^{-9}}{1+0.2q^{-1}-0.2q^{-2}} & \frac{0.01q^{-6}-0.03q^{-7}}{1+0.02q^{-1}-0.02q^{-2}} \\ \frac{-0.02q^{-7}-0.02q^{-8}}{1+0.01q^{-1}-0.01q^{-2}} & \frac{-0.2q^{-8}-0.3q^{-9}}{1+0.1q^{-1}-0.2q^{-2}} \end{bmatrix} \tag{30}$$

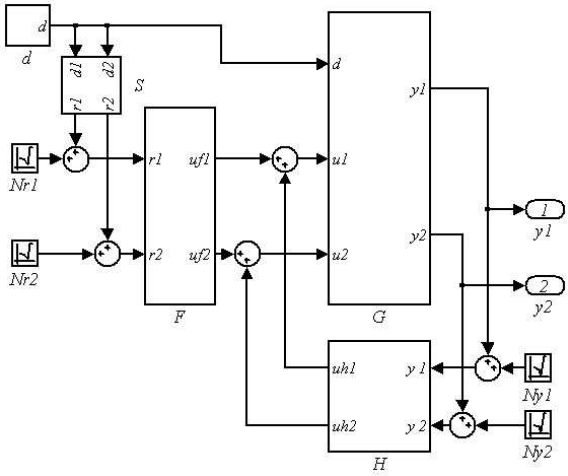

Fig. 8. SIMULINK® block diagram.

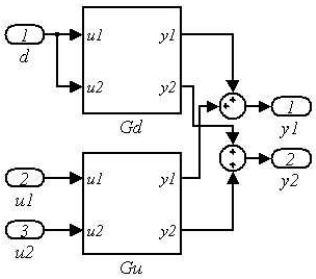

Fig. 9. SIMULINK® block diagram of Plant G.

and

$$G_d(q) = \begin{bmatrix} \frac{0.85q^{-4}}{1+0.4q^{-1}} & 0 \\ 0 & \frac{0.95q^{-6}}{1-0.2q^{-2}} \end{bmatrix} \tag{31}$$

The sampling frequency is 4kHz. The disturbance signal $\boldsymbol{d}$ is a mix of three sine-waves with frequencies of 50Hz, 80Hz and 100Hz and a white noise signal w_t with variance $1e-4$, leading to:

$$d(t) = \frac{1}{3}[\sin(100\pi t) + \sin(160\pi(t-0.091)) + \sin(200\pi t)] + w_t \tag{32}$$

The uncontrolled output is shown in Fig. 10.

The reference signal $r(t)$ is obtained from $d(t)$ by S:

$$S(q) = \begin{bmatrix} \frac{0.8q^{-8}}{1+0.8q^{-1}} & 0 \\ 0 & \frac{0.5q^{-10}}{1+0.9q^{-1}} \end{bmatrix} \tag{33}$$

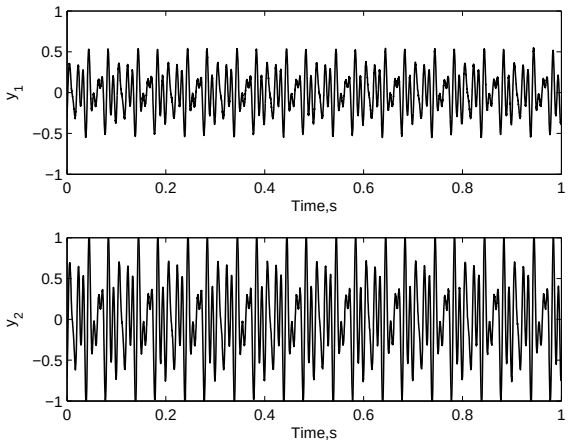

Fig. 10. Initial output without control.

6.2 *Simulation for FIR-FD-IT and FSF-FD-IT*

In this subsection two formats of controller structures are tested in simulation.

One is the FIR controllers (FIR-FD-IT) in which the feedback controller is 10-th order and feed-forward controller is 40-th order. The adaptation gain for the feed-forward controller tuning step is $\mu_f = 0.1$ and for feedback controller tuning it is $\mu_h = 0.02$.

The second controller format is FSF-FD-IT in which 1st-order Butterworth bandpass filters are applied in realtime according to the spectrum of $\boldsymbol{y}$. The bandwidths of the FSF are given by the disturbance frequency ± 10 percent which also eliminates the unwanted white noise in the tuning. The step size (adaptation gain) for feed-forward controller tuning is $\mu_f = 8.0$ and the step size for feedback controller tuning is $\mu_h = 2.0$.

The signal period is defined as $N = 800$. The length of tuning is set to 50 periods. All the initial controllers are set to zero. The weighting matrix is $Q = \text{diag}([1.0\,0.8])$. The initial performance criterion without control is 0.2443. In order to perform initial estimate of G, only the sub-block from $\boldsymbol{r}_1$ to $\boldsymbol{u}_{f1}$ in H is changed to 0.2 in the 2nd iteration, and only the sub-block from $\boldsymbol{r}_2$ to $\boldsymbol{u}_{f2}$ in H is changed to 0.2 in the 3rd iteration.

Fig. 11 is the update of performance in FIR-FD-IT: The 2nd and 3rd iteration are manual updates, which give $J(2) = 0.2432$ and $J(2) = 0.2391$. After 50 iterations, the final performance is $J = 0.0371$ with 8.2dB cancellation. The final output with control is shown in Fig.12.

Fig. 13 displays the performance updates in FSF-FD-IT. After 50 iterations, the final performance is $J = 0.0026$ with 19.8dB cancellation. The final output with control is shown in Figure14.

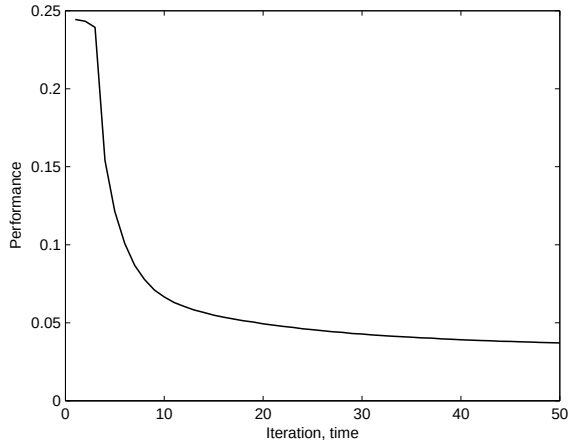

Fig. 11. Performance update in FIR-FD-IT .

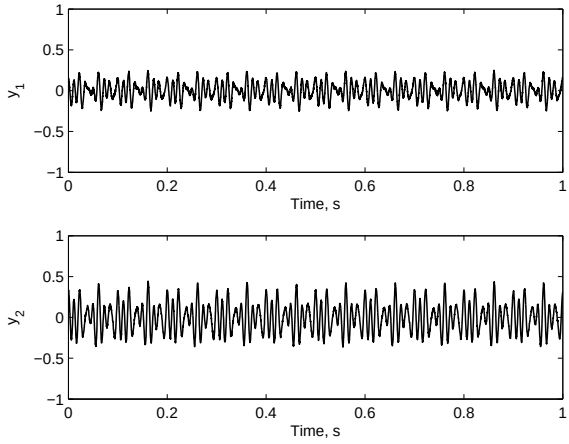

Fig. 12. Final output of FIR-FD-IT .

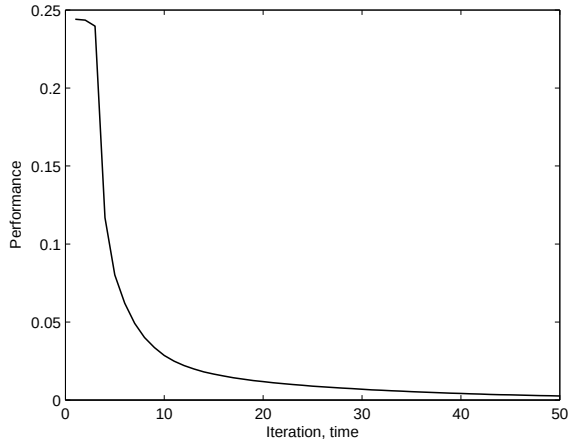

Fig. 13. Performance update in FSF-FD-IT .

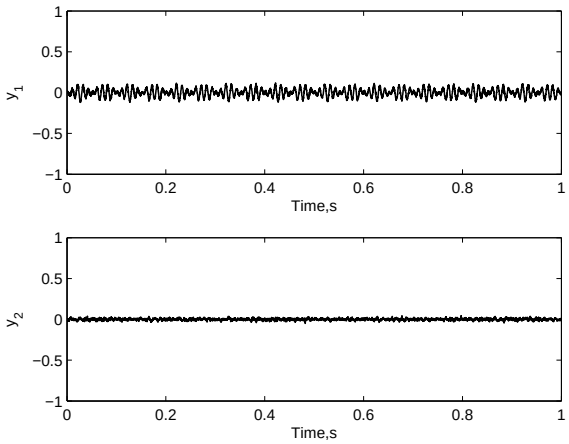

Fig. 14. Final output of FSF-FD-IT .

In comparison with FIR-FD-IT, FSF-FD-IT resulted in better tuning performance than FIR-FD-IT. The reason is that in FIR-FD-IT, given n_F-th order FIR for F and n_H-th order FIR for H, the tuning is performed in the n_F-dimensional space for F and n_H-dimension space for H. In FSF-FD-IT, FSF can split the whole solution space into independent n_ω sub-spaces since the FRF is independent in the LTI system. Each sub-space is 2-dimensional for the norm and phase of the complex gain. Therefore, the tuning is more effective in FSF-FD-IT.

6.3 Simulation for robustness against the errors in N

While the error of the frequency estimate from the finite time data is inevitable, the robustness against an error in N is important for FD-IT applications. To test the robustness against error in the frequency estimate, a series of simulations based on FSF-FD-IT were performed with varying data length N in (3).

In the above simulation the actual common period is $N = 800$. Given some estimation error N_e this period becomes $\hat{N} = N + N_e$. A series of simulation experiments are performed by changing $\hat{N}$ from 702 to 808, so that there are 4 experiments for each $\hat{N}$. In the test, $\mu_f = 4.0$ and $\mu_f = 1.0$.

Fig. 15 gives the change of the average final performance after 40 iterations when the estimated common period $\hat{N}$ changes from 795 to 805. According to above simulation results, FSF-FD-IT provides a fair amount of robustness to errors in disturbance period.

7 Conclusions

A frequency domain iterative feedback tuning approach has been presented that uses an innovative way of approximating gradient estimates of the controller cost function. The method is ideally suitable for ANVC applications with periodic disturbances. First gradient approximation has been

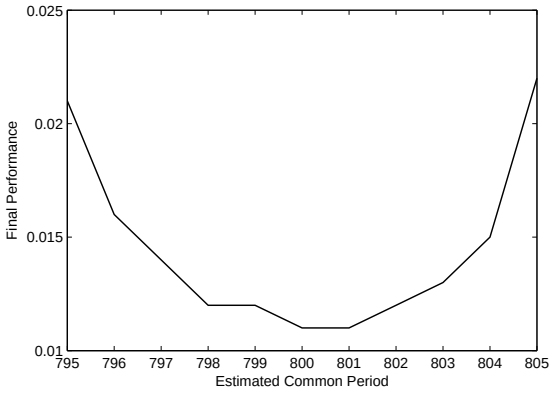

Fig. 15. Change of final performance with respect to $\hat{N}$

proposed in the frequency domain and an iterative tuning method has been developed for linear systems. Comparison has been made between the presented frequency domain and other published iterative tuning methods that has shown favourable properties of the new method proposed in terms of reduced number of experiments. The effectiveness, flexibility and robustness of the new method has been shown in simulation examples.

Future work is concerned with theoretical robustness analysis in the frequency domain. Extension of this general framework to other control application besides ANVC also requires further research.

References

[1] W. Edmonson, J. Principe, K. Srinivasan, and Chuan Wang. A global least mean square algorithm for adaptive iir filtering. *IEEE Circuits and Systems II*, 45(3):379 – 384, March 1998.

[2] S. J. Elliott and B. Rafaely. Frequency-domain adaptation of feedforward and feedback controllers. In *Proc. ACTIVE'97*, pages 75–92, 1997.

[3] H. Hjalmarsson. Efficient tuning of linear multivariable controllers using iterative feedback tuning. *Int. J. Adaptive Control and Signal Processing*, 13:553–572, 1999.

[4] H. Hjalmarsson. Iterative feedback tuning - an overview. *Int. J. Adaptive Control and Signal Processing*, 16:373 – 395, 2002.

[5] H. Hjalmarsson. From experiments to closed loop control. In *15th World Congress on Automatic Control*, 2003.

[6] H. Hjalmarsson and M Gevers. Algorithms and applications of iterative feedback tuning. *Special Section in Control Engineering Practice*, 11:1021, 2003.

[7] H. Hjalmarsson and Lequin O. Gevers M. Iterative feedback tuning: theory and applications. *IEEE Control Systems Magazine*, 18(4):26–41, 1998.

[8] H. Jansson and H. Hjalmarsson. Gradient approximations in iterative feedback tuning for multivariable processes. *Int. J. Adaptive Control and Signal Processing*, 18(8):665–681, 2004.

[9] H. Jansson, H. Hjalmarsson, and A. Hansson. On methods for gradient estimation in IFT for MIMO systems. In *15th World Congress on Automatic Control*, 2002.

[10] L. C. Kammer, R. R. Bitmead, and P. L. Bartlett. Direct iterative tuning via spectral analysis. *Automatica*, 36(9):1301–1307, 2000.

[11] A. Karimi, L. Mikovi, and D. Bonvin. Iterative correlation-based controller tuning: application to a magnetic suspension system. *Control Engineering Practice*, 11:1069–1087, 2003.

[12] J. Luo and S.M. Veres. Iterative feedback/feedfoward tuning control in the frequency domain for AVNC. In *European Control Conference 2007, ECC'07*, page 381C388, Kos, Greece, 2007. EUCA.

[13] J. Luo and S.M. Veres. Frequency domain iterative tuning for the control of nonlinear vibrations. In *Proceedings of the 47rd IEEE conference on decision and control, CDC'08*, pages 3014–3019, Cancun, Mexico, 2008. IEEE.

[14] J. Luo and S.M. Veres. MIMO frequency domain iterative tuning for tracking control. In *Proceedings of 17th IFAC World Congress*, pages 451–456, Seoul, Korea, 2008. Elsevier.

[15] T. Meurers. *Self-tuning and adaptive controllers for active sound and vibration control*. PhD thesis, School of Engineering Science, University of Southampton, 2002.

[16] T. Meurers and S. M. Veres. Iterative design for vibration attenuation. *Int. J. Acoustics and Vibration*, 4(2):79–83, 1999.

[17] T. Meurers, S. M. Veres, and S. J. Elliott. Frequency selective feedback for active noise control. *Control System Magazine, IEEE*, 22:32 – 41, Aug. 2002.

[18] D. R. Morgan. An analysisi of multiple correlation cancellation loops with a filter in the auxiliary path. *IEEE Trans. on Acoustics, Speech and Signal Processing*, 28(4):454–467, 1980.

[19] A. V. Oppenheim and A. S. Willsky. *Signals and Systems*. Prentice Hall, 2nd edition, 1996.

[20] R. H. J. M. Otten and L. P. P. P. van Ginneken. *The Annealing Algorithm*. Kluwer Academic Pulisher, 1989.

[21] P. M. Pardalos and J. B. Roseb. *Contstrained Global Optimization: Algorithms and Applications*. Springer-Verlag, 1987.

[22] Ning Qian. On the momentum term in gradient descent learning algorithms. *Neural Networks*, 12(1):145–151, 1999.

[23] S. M. Veres and H. Hjalmarsson. Tuning for robustness and performance using iterative feedback tuning. *42nd IEEE Conference on Decision and Control*, 4:4682 – 4687, 2002.

[24] S. M. Veres and D. S. Wall. *Synergy and duality of identification and control*. Taylor & Francis, London, 2000.